Intracellular pH Regulation during Spreading of Human Neutrophils

Nicolas Demaurex,* Gregory P. Downey,‡ Thomas K. Waddell,‡ and Sergio Grinstein*

*Division of Cell Biology, The Hospital for Sick Children, Toronto M5G 1X8, Canada; ‡Division of Respiratory Diseases, Institute of Medical Sciences, Department of Medicine, the University of Toronto, M5S 1A8, Canada

Abstract. The regulation of the intracellular pH (pH_i) during spreading of human neutrophils was studied by a combination of fluorescence imaging and video microscopy. Spreading on adhesive substrates caused a rapid and sustained cytosolic alkalinization. This pH_i increase was prevented by the omission of external Na^+, suggesting that it results from the activation of Na^+/H^+ exchange. Spreading-induced alkalinization was also precluded by the compound HOE 694 at concentrations that selectively block the NHE-1 isoform of the Na^+H^+ antiporter. Inhibition of Na^+/H^+ exchange by either procedure unmasked a sizable cytosolic acidification upon spreading, indicative of intracellular acid production. The excess acid generation was caused, at least in part, by the activation of the respiratory burst, since the acidification closely correlated with superoxide production, measured in single spreading neutrophils with dihydrorhodamine-123, and little acid production was observed in the presence of diphenylene iodonium, a blocker of the NADPH oxidase. Moreover, neutrophils from chronic granulomatous disease patients, which do not produce superoxide, failed to acidify. Comparable pH_i changes were observed when β2 integrins were selectively activated during spreading on surfaces coated with anti-CD18 antibodies. When integrin engagement was precluded by pretreatment with soluble anti-CD18 antibody, the pH_i changes associated with spreading on fibrinogen were markedly reduced. Inhibition of microfilament assembly with cytochalasin D precluded spreading and concomitantly abolished superoxide production and the associated pH_i changes, indicating that cytoskeletal reorganization and/or an increase in the number of adherence receptors engaged are required for the responses. Neutrophils spread normally when the oxidase was blocked or when pH_i was clamped near physiological values with nigericin. Spreading, however, was strongly inhibited when pH_i was clamped at acidic values. Our results indicate that neutrophils release superoxide upon spreading, generating a burst of intracellular acid production. The concomitant activation of the Na^+/H^+ antiport not only prevents the deleterious effects of the acid released by the NADPH oxidase, but induces a net cytosolic alkalinization. Since several functions of neutrophils are inhibited at an acidic pH_i, the coordinated activation of pH_i regulatory mechanisms along with the oxidase is essential for sustained microbicidal activity.

THE microbicidal activity of neutrophils depends on their ability to emigrate from the vascular space, a process that requires remarkable cellular plasticity: the circulating spherical cells must rapidly spread to promote their firm adhesion to the endothelium and become polarized to facilitate transmigration. Neutrophil spreading can be induced by a variety of soluble and substrate-bound stimuli (15, 30) that initiate a highly coordinated cascade of events leading to the reorientation of the actin cytoskeleton (14, 38) and promote receptor-mediated adhesion of neutrophils to surfaces such as the endothelium (15).

The intracellular signals associated with neutrophil spreading are largely unknown, in part because their study necessitates dynamic measurements of high temporal and spatial resolution in living cells. Recent advances in fluorescence microscopy and the development of indicator dyes have allowed the measurement of the intracellular concentration of biologically active compounds in single motile cells (41). In phagocytes, such studies have focused almost exclusively on the intracellular free Ca^{2+} concentration, $[Ca^{2+}]_i$[1] because of the perceived importance of this ion in regulating cellular functions such as cytoskeletal reorganization, cell motility, and secretion (3, 31). Indeed, several groups have reported that leukocyte motility correlates spatially and temporally with changes in $[Ca^{2+}]_i$ (6, 25, 26, 28, 29, 39). However, the role of other potentially important signaling events has not been investigated in comparable detail.

Please address all correspondence to Dr. Nicolas Demaurex, Division of Cell Biology, Hospital for Sick Children, 555 University Avenue, Toronto M5G 1X8. Tel.: (416) 813-5727; Fax: (416) 813-5028.

1. *Abbreviations used in this paper:* BCECF, 2′7′*bis*-(2-carboxyethyl)-5 (and -6) carboxyfluorescein; $[Ca^{2+}]_i$, intracellular free Ca^{2+} concentration; CGD, chronic granulomatosus disease; DHR, dihydrorhodamine 123; DPI, diphenylene iodonium; fMLP, *N*-farmyl-L-methionyl-L-leucyl-L-phenylalanine; NHE, Na^+/H^+ exchanger; NMG, *N*-methyl-D-glucammonium.

Cytosolic pH (pH_i) is a candidate to regulate cell motility, since certain steps in the actin polymerization sequence and the binding of actin filaments to membrane-anchoring proteins are pH-dependent events (17). Indirect observations are consistent with this notion: the ability of neutrophils to polarize and perform chemotaxis is reduced when the extracellular pH (pH_o) is made acidic, which is expected to lower pH_i (35). More importantly, it is possible to induce cytoskeletal reorganization in neutrophils in a receptor-independent manner by the addition of weak electrolytes, which can modify pH_i at constant pH_o (35). Therefore, pH_i must be given consideration as a regulator and possible mediator of cell spreading and chemotaxis.

Like most cells, resting neutrophils maintain their pH_i within a narrow physiological range by regulating the rate of net H^+ flux across the plasma membrane. Particularly efficient H^+ extrusion systems are required when neutrophils are activated, to compensate for the acid produced by the NADPH oxidase, an enzymatic complex that generates microbicidal superoxide anions (2, 8). Two intracellular acid equivalents are released for every superoxide ion that is produced, and additional acid is formed during the resynthesis of NADPH by the hexose monophosphate shunt (4). Accordingly, stimulation of suspended neutrophils by chemoattractants is associated with a burst of intracellular acid production and a concomitant increase in H^+ efflux (21, 24). While increased H^+ extrusion approaches the rate of H^+ generation, the coupling of these processes is not stoichiometric, leading to readily measurable pH_i changes during neutrophil activation (22, 34). Such deviations from the resting pH_i might, in turn, influence the organization of the actin cytoskeleton and hence modulate other cellular processes such as spreading and motility. To gain insight into these interactions, we used fluorescence ratio imaging combined with phase-contrast video microscopy to measure changes in pH_i during the spreading of human neutrophils.

Materials and Methods

Materials and Media

Heparin was obtained from Organon Teknika (Toronto, ON). Dextran T500 and Percoll were purchased from Pharmacia (Milwaukee, WI). Krebs-Ringer phosphate-buffered medium (KRPD) was prepared using reagents from Mallinckrodt (Paris, KY). *N*-methyl-D-glucammonium (NMG) medium contained (in mM) 140 NMG chloride, 3 KCl, 1 $MgCl_2$, 1 $CaCl_2$, 10 glucose, and 20 Hepes, titrated to pH 7.5 at 37°C. Nigericin, dihydrorhodamine 123 (DHR), as well as the acetoxymethyl ester forms of 2′7′ *bis*-(2-carboxyethyl)-5 (and -6) carboxyfluorescein (BCECF) and of Indo-1 were purchased from Molecular Probes, Inc. (Eugene, OR). Cytochalasin D and fibrinogen were purchased from Sigma Immunochemicals (St. Louis, MO). The mAb IB4 was a kind gift from Dr. David Chambers (San Diego Regional Cancer Center, San Diego, CA), anti–glutathione *S*-transferase mAb was from Santa Cruz Biotechnology Associates (Santa Cruz, CA). All other chemicals, of analytical grade, were from Aldrich Chemical Co. (Milwaukee, WI). Compound HOE 694 was a generous gift from Hoechst (Zürich, Switzerland). Diphenylene iodonium (DPI) was synthesized in our laboratory as described (9).

Cells

Human neutrophils (>98% pure) were isolated from heparinized or citrated whole blood obtained by venipuncture, using dextran sedimentation and discontinuous plasma-Percoll gradients as described (5). The same procedure was used to obtain neutrophils from a chronic granulomatous disease (CGD) patient with a deletion in the gene encoding $gp91^{phox}$, which resulted in the complete absence of glycoprotein expression. After isolation, cells were resuspended in KRPD buffer at 8×10^6/ml and kept at room temperature on a rotating wheel until used (generally <3 h). For fluorescence measurements, 1-ml aliquots of this suspension were incubated for 5–10 min with 2 μM of the acetoxymethyl ester form of the pH-sensitive dye BCECF. Glass coverslips (Thomas Scientific, Swedesboro, NJ), either noncoated or coated with antibodies or fibrinogen as described (3), were inserted into a thermostated perfusion chamber (Open Perfusion Micro-Incubator; Medical Systems Corp., Greenvale, NY) Placed on the stage of an inverted microscope. The objective was focused on the upper surface of the coverslip, and 1 ml of the appropriate solution was added to the chamber. A 100-μl aliquot of the suspension of BCECF-loaded neutrophils (10^6 cells) was then gently added, and image acquisition was started immediately upon contact of the neutrophils with the glass surface. All experiments were performed at 37°C.

Video Microscopy and pH Imaging

Simultaneous imaging of cellular BCECF fluorescence and cell morphology was performed by a method similar to that described by Foskett (19), using an inverted microscope (Diaphot TMD; Nikon Canada, Toronto, ON) equipped with epifluorescence optics. Alternate excitation of BCECF at 490 and 440 nm was provided by a computer-controlled shutter and filter wheel assembly (Metaltek; Empix Imaging, Toronto, ON), while continuous 620-nm illumination was achieved by filtering the transmitted incandescent source. The 440/490-nm light was reflected to the cells by an excitation dichroic mirror (510 nm), and the emitted fluorescence (>510 nm) and the transmitted red light (>620 nm) were separated by an emission dichroic mirror (565 nm). The red light was directed to a video camera, allowing continuous visualization of the cells, while the fluorescent light was directed onto a 535 ± 25-nm filter and imaged with a slow-scan, cooled (−45°C) CCD camera (Star-1; Photometrics, Tucson, AZ). The large separation between the fluorescence and bright field signals (535 and 620 nm) resulted in no measurable "cross-talk" between the two light paths, and allowed continuous assessment of cell morphology without interfering with the fluorescence measurements. The bright fluorescence of BCECF at both excitation wavelengths (440 and 490 nm) and the use of high transmission objectives (NA = 1.3–1.4) allowed short exposure times (typically 0.5 s), enabling us to maintain a <3 s interval between fluorescence image pairs to minimize motion artefacts. The size of the CCD array imaged was chosen to match the optics so that, on average, 10 neutrophils fit within the digital image. Low resolution images were obtained with a 40× objective (Nikon) and ~1/8 of the CCD array, while high resolution images were obtained with a 63× objective (Zeiss, Oberkochen, Germany) and ~1/4 of the CCD array. Low resolution images were used for rapid acquisition with minimal illumination (see below), whereas high resolution images were obtained mainly for illustration purposes in combination with bright-field images. Control of image acquisition and of the excitation filter selection was achieved using the Metafluor software (Universal Imaging Corp., West Chester, PA) running on a computer (486-66; Dell Inc., Mississauga, Canada) interfaced to the Photometrics camera via a 12-bit GPIB II/IIA board (National Instruments, Foster City, CA).

Calibration and Photodynamic Considerations

At the end of each experiment, a calibration curve of fluorescence ratio vs. pH was obtained in situ by sequentially perfusing the cells with 5 μM nigericin KCl-rich media buffered at four different pH values ranging from 6.0 to 7.5, as described (40).

When a high intensity excitation light (440/490 nm) was used, it was noted that the illuminated neutrophils failed to spread and they acidified rapidly, whereas nonilluminated neutrophils on the same coverslip spread normally. This suggested that upon intense illumination of BCECF, photodynamic damage occurred which interfered with normal neutrophil function. To minimize such damage, the excitation light was attenuated 100-fold (neutral density 2 filter) and the interval between ratio images was increased to 12 s. Under these conditions, the degree of spreading of illuminated neutrophils was >90% of nonilluminated controls.

Image Processing

The 490- and 440-nm fluorescence images were corrected for shading to compensate for uneven illumination, the background was subtracted, and a threshold of five times the value of the background noise (RMS) was applied before obtaining a pixel-by-pixel ratio of the two images. Subthresh-

old pixels were neither displayed nor used for subsequent analysis to prevent artefacts caused by ratioing near-zero values. The resulting ratio images were displayed on-line, and regions of interest (ROI) encompassing the cells were defined. The averaged ratio values of the ROI were calculated and plotted to follow the kinetics of the pH_i changes throughout an experimental period. Cellular area and ellipsoidicity were calculated by manually tracing the cells on the acquired digital images. The "shape factor" or ellipsoid is a geometrical, two-dimensional parameter that indicates deviation from a circular (value = 1) to a noncircular shape (value <1) (26, 27). The shape factor was calculated as $= 4\pi \times$ area/(perimeter)^2, using the values measured from the digital images (in pixels). Because round cells contributed more out-of-focus fluorescence, they appeared larger on the fluorescence images than on the corresponding bright field images. Conversely, thin, spread cells appeared smaller on the fluorescence image because low intensity pixels near the cell edge were eliminated by the threshold correction. Morphological parameters were derived from bright-field images, since these more precisely reflected the shape changes associated with neutrophil spreading. Composite figures were created by superimposing the ratio images over the corresponding transmitted images, which were acquired on the same camera, using Adobe Photoshop 3.0 software (Adobe Systems Inc., Mountain View, CA).

Superoxide Measurements

Superoxide production was measured in single neutrophils using DHR. The cells were allowed to adhere for 1 min in a solution containing 2 μM DHR, and were then perfused throughout the experiment with a similar DHR-containing solution to minimize the contribution of extracellular rhodamine 123. In some experiments, CGD neutrophils were loaded with Indo-1 by incubating for 30 min at 37°C with 2 μM of the precursor acetoxymethyl ester. The fluorescence of rhodamine 123, the oxidized product of DHR and of Indo-1, were measured on the optical system described above, using 360-nm (Indo) and 490-nm (rhodamine 123) excitation filters and the 535 ± 25-nm emission filter used for BCECF.

Results

Cytosolic pH (pH_i) Changes during Neutrophil Spreading

The pH_i changes associated with neutrophil spreading

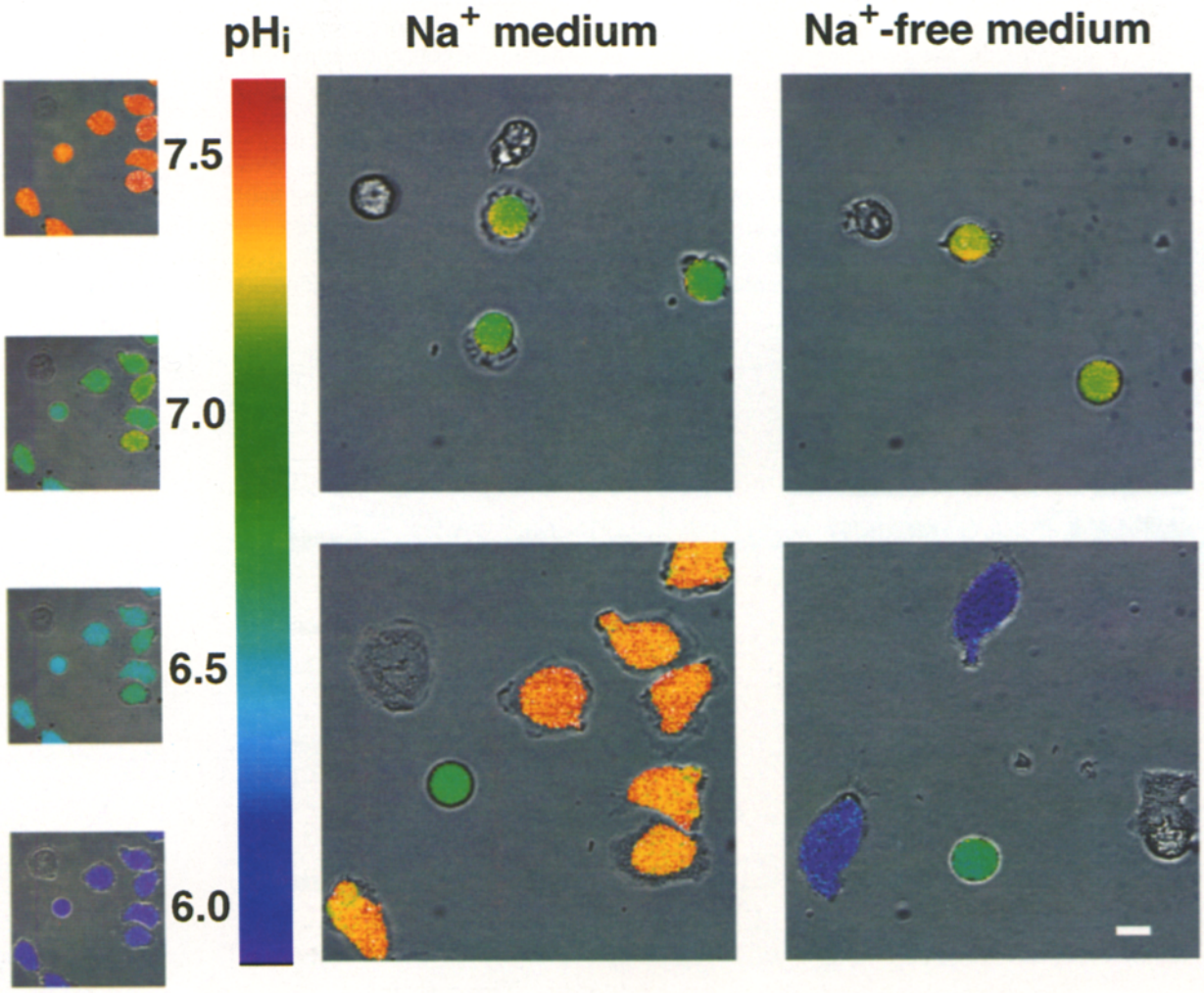

Figure 1. Spreading-associated pH_i changes in human neutrophils. Composite images of pH_i (in pseudocolor) and cell morphology (in black and white) during spreading of neutrophils on a glass surface. pH_i was estimated from the excitation ratio of BCECF fluorescence, as described under Materials and Methods. The pH_i images have been superimposed on bright-field, phase-contrast images acquired ~10 s later with the same camera. Some cells have been left unmasked to better illustrate their morphology. (*Main panels*) Neutrophils adhered for 1 min (*top*) and 20 min (*bottom*) in standard saline solution (*left*) or in nominally Na^+-free solution (*right*). (*side panels*) The cells shown in the main panel at bottom left were calibrated by sequential perfusion with nigericin-containing solutions at the indicated pH. Note that in the presence of nigericin, the pH_i measurements are not affected by the degree of cellular spreading. Bar, 5 μm.

were investigated by a combination of phase-contrast and fluorescence ratio imaging. Freshly isolated blood neutrophils were allowed to settle randomly on a coverslip at the bottom of the microscope chamber, and nonadherent cells were removed by gentle solution exchange before initiating image acquisition (1 min after plating). Fig. 1 illustrates a typical experiment in which fluorescence ratio images (converted to pH_i and scaled in pseudocolor) have been superimposed on transmitted bright-field images. Pseudocolor images were omitted from some cells for optimal illustration of their morphology. Shortly after adherence, the pH_i value of neutrophils was close to 7.0 (Fig. 1, $t = 1$ min) and was similar in Na^+-containing medium (Krebs-Ringer solution) and in Na^+-free medium, where Na^+ was replaced by *N*-methyl-D-glucammonium (NMG). Most of the cells, which were initially spherical, rapidly extended lamellipodia in both types of media. Within 5 min, the majority of the cells had spread and were observed to migrate randomly on the coverslip. After 20 min, >90% of the cells displayed spreading, which was associated with sizable changes in pH_i. Interestingly, these changes in pH_i were in opposite directions in Na^+-containing and Na^+-free solutions (Fig. 1, $t = 20$ min): in the presence of Na^+, cell spreading was associated with a cytosolic alkalinization of ~0.2 pH units, whereas in Na^+-free medium, a marked cytosolic acidification (~0.8 pH) was observed. In any given medium, all spreading neutrophils displayed similar changes in pH_i, and no significant differences were observed between motile and stationary cells. However, neutrophils migrated more actively and for longer periods of time when bathed in Na^+-free medium. In Na^+-containing medium, cells tended to flatten and became immobile earlier. In contrast to the large changes in pH_i observed in spreading cells, the small fraction of neutrophils that adhered but did not spread displayed only a modest cytosolic acidification both in Na^+-containing and Na^+-free media (Fig. 1, round cells at $t = 20$ min). Similar observations were made in neutrophils obtained from 15 different donors (353 cells in Na^+ medium and 121 cells in NMG^+ medium).

In all cells studied, the measured pH_i appeared to be homogeneous throughout the cytosol, and no pH gradients or microdomains were observed. It was important, however, to ascertain that the pH_i changes recorded upon spreading were not artifactual, perhaps resulting from changes in the focal plane, reduced fluorescence signals caused by thinning of the layer of BCECF under observation, or abnormal interactions of the dye with cellular components such as the cytoskeleton, which undergo remodeling during cell spreading and migration. These concerns were addressed by treating cells with nigericin in a K^+-rich medium. Under these conditions, because the intra- and extracellular concentrations of K^+ are nearly identical, the ionophore is expected to equalize the cytosolic and external concentrations of H^+. As illustrated in the left column of Fig. 1, the pH_i of adherent neutrophils could indeed be readily manipulated with nigericin/K^+, and this procedure was used for calibration of fluorescence ratio vs. pH_i. More importantly, in the presence of the ionophore, the differences that were noted between round and spread cells were consistently eliminated, with homogeneous fluorescence ratios observed at both optimal and suboptimal focal planes. These observations rule out the possibility of

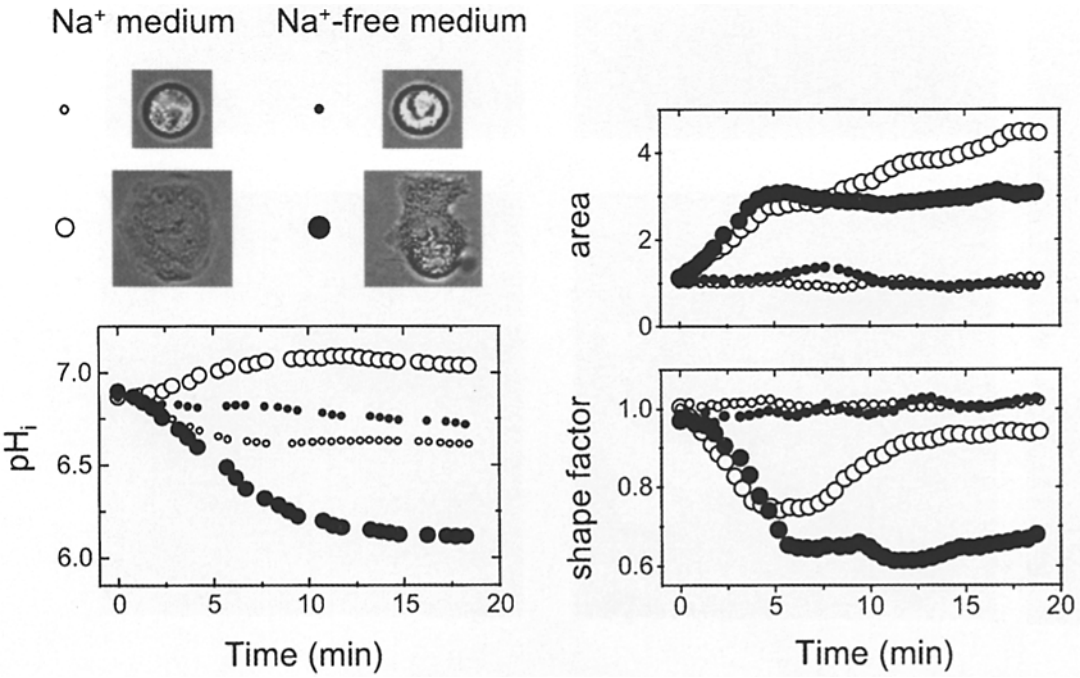

Figure 2. Time course of pH_i and shape changes during neutrophil spreading on glass. Changes in pH_i (*left panel*), cellular area (*top right*), and shape factor (deviation from circular geometry, *bottom right*) were monitored over time in adherent cells. Representative cells (the non-masted cells in Fig. 1) are illustrated in the left inset. Two cells that underwent spreading (*large circles*) and two that remained round throughout the experiment (*small circles*) are shown. Cells incubated in Na^+-containing (*open circles*) and Na^+-free medium (*filled circles*) are compared. Cellular area and shape factor were determined by manually tracing the cell perimeter of the digital images. Time courses are representative of 174 cells from 34 experiments.

optical artifacts, and they imply that the pH_i changes associated with neutrophil spreading are genuine.

Fig. 2 illustrates the temporal correlation between the changes in pH_i (*left panel*) and in cell shape (*right panels*) of representative neutrophils (*insets*). Cells that underwent spreading (Fig. 2, *large symbols*) are compared to cells that remained round throughout the experiment (Fig. 2, *small symbols*). The changes in pH_i associated with spreading in Na^+-containing (Fig. 2, *open circles*) and Na^+-free media (Fig. 2, *filled circles*) followed similar time courses, reaching completion after 10 min. Cellular shape alterations and spreading clearly preceded these pH_i changes, as is apparent from the time courses of two geometrical parameters: cellular "area" (Fig. 2, *top right*) and "shape factor" (Fig. 2, *bottom right*). The surface area was estimated by outlining the perimeter of the cell at the focal plane, and directly measured the extent of cellular spreading. The shape factor or ellipsoid is a geometrical parameter that indicates deviation from a circular (value ~1) to a more elongated shape (value <1; see Materials and Methods). The ellipsoid measures the degree of cellular asymmetry but does not distinguish between spread and nonspread cells. As expected, nonspread cells maintained constant area and ellipsoid values throughout the experiment, whereas a three to fourfold increase in area was observed in spread cells that assumed a variety of shapes, yielding ellipsoid values ranging from 0.5 to 1.0 (Fig. 2, *right panels*). The initial pseudopod extension was readily detected as increases in both area and cell asymmetry (i.e., a decrease in shape factor). These shape changes were complete within 5 min, with similar time courses in Na^+-containing and Na^+-free medium. After this initial spreading phase, however, the cells behaved differently, depending on the composition of the bathing medium. In the Na^+-containing solution, the neutrophils continued to flatten and assumed a near-circular geometry, as detected by the continuous increase in area and the return to ellipsoid values near 1. In contrast, in Na^+-free medium, the cells maintained a constant area and remained asymmetrical until the end of the recording (~20 min).

Neutrophil spreading on physiological substrates is mediated primarily by the adherence receptors of the β2-integrin family (37). These receptors, which share a common β chain (CD18), most likely participate in the rapid spreading of neutrophils on glass. Other undefined adherence receptors, however, may participate as well. To assess the involvement of β2 integrins, these were either selectively engaged by coating coverslips with anti-CD18 mAb (IB4), or their activation was prevented by preincubation with soluble anti-CD18. Fig. 3 *A* shows that neutrophils spread rap-

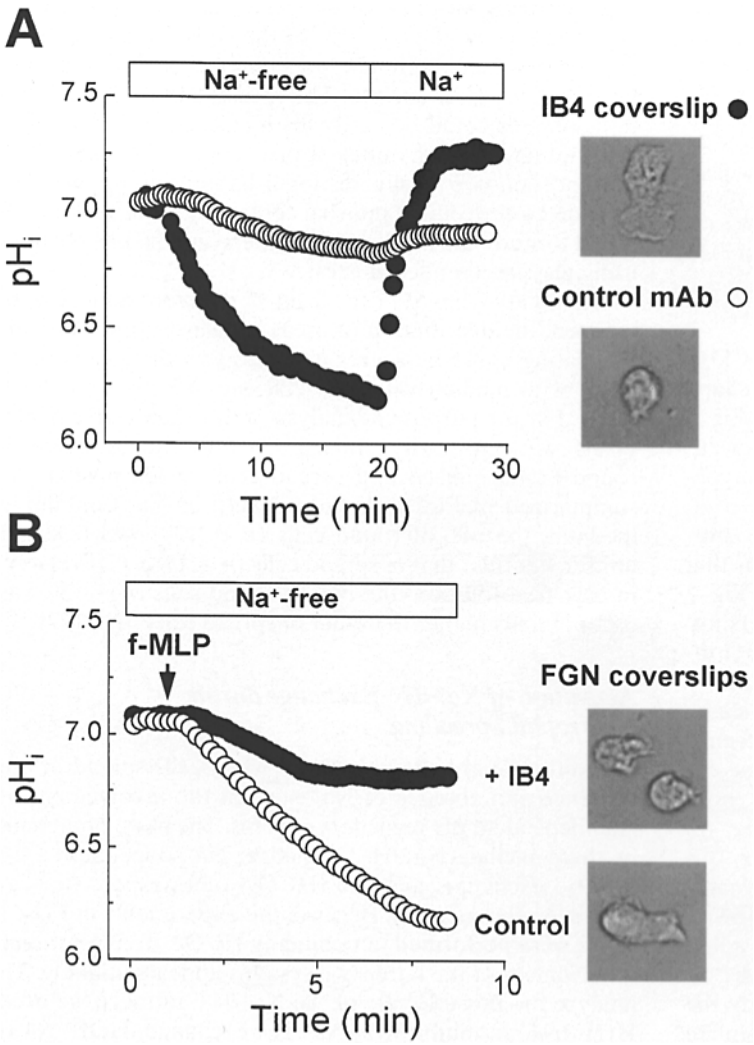

Figure 3. Integrin-mediated spreading and pH_i changes. pH_i changes during adherence and spreading on coverslip coated with anti integrin mAb or fibrinogen. (*A*) Cells were suspended in Na^+-free medium and allowed to adhere to coverslips coated with either an anti-CD18 mAb (*filled circles*) or an isotype-matched control mAb (*open circles*), and pH_i was measured as described in Fig. 1. Where indicated, the Na^+-free solution was changed to an Na^+-containing solution. (*B*) Cells suspended in Na^+-free medium were allowed to adhere to fibrinogen-coated coverslips in the presence (*filled circles*) or absence (*open circles*) of soluble IB4 mAb. Where indicated, 10^{-7} M fMLP was added. Data are means from three to five cells from one representative experiment; insets illustrate the typical morphology that was observed in each condition.

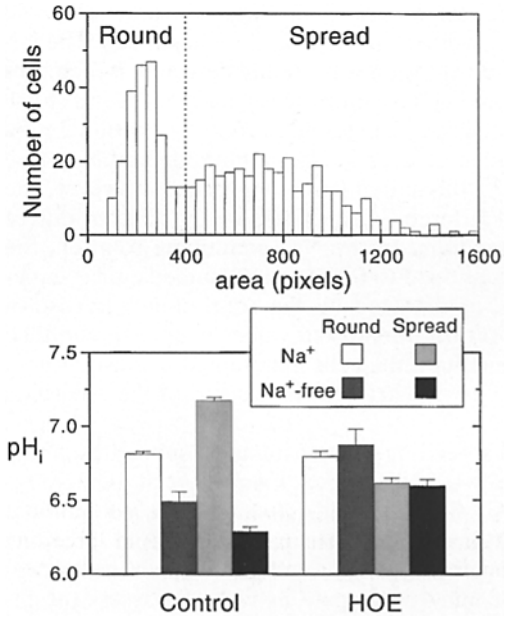

Figure 4. Na^+/H^+ exchange in aherent and spread neutrophils. (*Top panel*) Frequency distribution of the surface area of neutrophils 10–20 min after plating on glass. The cell areas (n = 517) were traced on the fluorescence images, as detailed under Materials and Methods. Because pixels near the cell edges are below the threshold set for acquisition of the fluorescence images (see Materials and Methods), this procedure underestimates the spreading-induced changes in the area. Neutrophils were arbitrarily separated into spread and round cells, where indicated by the vertical line. (*Bottom panel*) Steady-state pH_i values of round and spread neutrophils, measured 10–20 min after adhesion in Na^+-containing or Na^+-free medium. Where indicated, the medium contained 1 μM HOE 694. The cells were separated into round and spread, using the criteria defined in the top panel. For each condition, data are means ± SEM of at least 50 cells from 3–12 experiments.

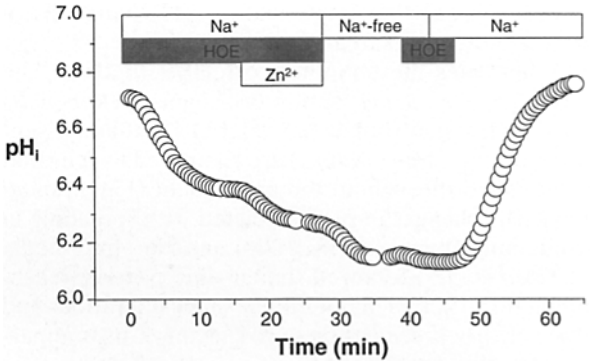

Figure 5. Block of Na^+/H^+ exchange unmasks a spreading-dependent acidification. Effect of Na^+/H^+ exchange inhibition on pH_i during spreading to glass coverslips. The cells were initially bathed in Na^+-rich medium containing 1 μM HOE 694 (see bars on top of figure). When indicated, the solution was supplemented with $ZnCl_2$ (2 mM), and then exchanged for a Na^+-free solution devoid of blockers. HOE 694 and Na^+ were subsequently reintroduced to assess the efficiency of the inhibitor. The data points are means of pH_i determinations in eight cells, all of which spread within 10 min of plating.

idly when plated on coverslips coated with the anti-CD18 mAb and that, as during adherence to glass, the shape changes were accompanied by massive pH_i changes (Fig. 3 *A*, *filled circles*). Only minor shape and pH_i changes were observed on coverslips coated with a control, isotype-matched mAb (anti–glutathione *S-transferase, Fig. 3 A, open circles*). Conversely, incubation with soluble anti-CD18 mAb prevented the responses observed in cells that were plated on a physiological matrix. As shown in Fig. 3 *B*, when cells were placed on fibrinogen-coated coverslips, stimulation with the chemoattractant fMLP (10^{-7} M) induced synchronous spreading that was accompanied by large pH_i changes (Fig. 3 *B*, *open circles*). Both the shape and pH_i changes were markedly reduced in the presence of soluble IB4 mAb (Fig. 3 *B*, *filled circles*). Thus, the engagement of β2 integrins is sufficient to induce both spreading and pH_i changes, and is required for the response to chemoattractants on a physiological matrix. It is noteworthy, however, that soluble IB4 mAb did not markedly alter the responses observed on glass (not shown), suggesting that additional ligands participate in the adhesion of neutrophils to this substrate. Glass, however, offered some advantages as a model substrate to study the pH_i changes associated with neutrophil spreading. Unlike fibrinogen, spreading did not require additional stimulation with soluble chemoattractants. On IB4-coated coverslips, virtually all the cells spread within minutes of plating, whereas on glass, ~30% of the cells remained round throughout the experiment, presumably because of irregularities of the glass surface. The spread and round populations of cells could be easily distinguished based on their area, integrated as number of pixels per cell (Fig. 4). The presence of two easily distinguishable cell populations provided a convenient internal control. For this reason, we opted to study the mechanisms underlying the pH_i changes using glass as a model substrate.

When data from 517 cells from 15 different donors were collated, the distribution of areas measured 10–20 min after plating could be segregated into two distinct populations, with median values of 228 and 783 pixels, respectively. For the purpose of analysis, a threshold value of 400 pixels was arbitrarily chosen to differentiate between round (<400 pixels) and spread cells (>400 pixels). As summarized in Fig. 4 (*bottom panel*), in Na^+-containing medium, the pH_i of round cells (n = 139) was 0.36 pH units lower than that of spread cells (n = 178). Conversely, in Na^+-free solution, the pH_i of round cells (n = 73) was 0.21 pH units higher than that of spread cells (n = 127).

Activation of Na^+/H^+ Exchange during Neutrophil Spreading

The differential behavior of pH_i when cells spread in the presence and absence of Na^+ suggest the involvement of Na^+-dependent pH regulatory systems. The more prominent of these include Na^+/H^+ exchange, Na^+-dependent Cl^-/HCO_3^- exchange, and $Na^-(HCO_3)_n$ cotransport (for review see reference 32). Because the experiments in Figs. 1 and 2 were performed in nominally HCO_3^--free solutions, involvement of the latter two systems appears unlikely. To analyze the possible role of the Na^+/H^+ antiport, we used HOE 694, an inhibitor of Na^+/H^+ exchange. HOE 694 is

not only a potent and selective inhibitor, but it has the additional advantage that it can be used to differentiate between isoforms of the Na^+/H^+ exchanger (NHE). The NHE-1 isoform is nearly 50-fold more sensitive to HOE 694 than NHE-2, which is in turn 100-fold more sensitive than NHE-3 (10). The susceptibility of NHE-4 and the recently identified NHE-5 to inhibition by this blocker has not been examined.

When neutrophils were plated in Na^+-containing medium supplemented with 1 μM HOE 694, adhesion and spreading proceeded normally. The presence of HOE 694, however, unmasked a sizable cytosolic acidification (Fig. 5) that contrasted with the alkalinization normally observed in the absence of the inhibitor (e.g., Fig. 2). This finding suggests that the Na^+-dependent increase in pH_i noted during neutrophil spreading in physiological solutions is mediated by activation of Na^+/H^+ exchange. Inhibition by 1 μM HOE 694 suggests involvement of NHE-1, consistent with the detection of this isoform in neutrophils by RT-PCR and immunochemical methods (20).

The cytosolic acidification observed in Na^+ medium in the presence of HOE 694 had a similar time course but was less pronounced than that in Na^+-free (NMG) medium (cf. Figs. 2 and 5). One possible explanation for this observation is that HOE 694 failed to inhibit Na^+/H^+ exchange completely at the concentration used. This possibility was discounted by the experiments in the latter part of Fig. 5. After drastic acidification of the cells in Na^+-free medium, reintroduction of Na^+ in the presence of 1 μM HOE 694 had no discernible effect on pH_i. Upon removal of the inhibitor, a robust alkalinization was recorded.

Alternatively, the excess acidification in Na^+-free medium could be explained by import of extracellular H^+ through reversal of the antiport, since under these conditions, the Na^+ concentration gradient is outward. This notion is supported by the finding that the acidification induced by cell spreading in NMG^+ medium was partially inhibited by HOE 694 (Fig. 4, *bottom panel*). Moreover, the magnitude of the acidification was not significantly different in Na^+-free vs. Na^+-containing media when HOE 694 was present. Together, these findings indicate that the blocker completely inhibited Na^+/H^+ exchange and that reversal of the activated antiport contributes to the acidification that is noted in Na^+-free medium.

Intracellular Acid Production and NADPH Oxidase Activation

The drastic acidification experienced by neutrophils while spreading in Na^+-free media is only partly caused by reversal of the NHE. A large component of the pH_i change persists in the presence of inhibitors of the antiport (Fig. 5), suggesting the generation of endogenous acid equivalents by metabolic pathways activated by adherence and/or spreading. Of particular relevance is the respiratory burst mediated by the NADPH oxidase, which has been shown to be associated with net acid generation (4) and which can promote intracellular acidification when suspended neutrophils are treated with phorbol esters (21). To assess the role of this pathway, we used neutrophils from CGD patients (Fig. 6) who are deficient in components of the NADPH oxidase and are therefore unable to produce superoxide (36). Although CGD neutrophils spread as well as control neutrophils (Fig. 6, *insets*), the acidification observed in Na^+-free medium was markedly reduced in the former (Fig. 6, *circles*), indicating that a functional NADPH oxidase is required for the acidification. Importantly, CGD and control neutrophils alkalinized with similar time courses upon Na^+ readdition, indicating that Na^+/H^+ exchange was activated in both cell types. CGD cells, however, reached a higher steady-state pH_i, as was expected if an offsetting acidification component had been eliminated.

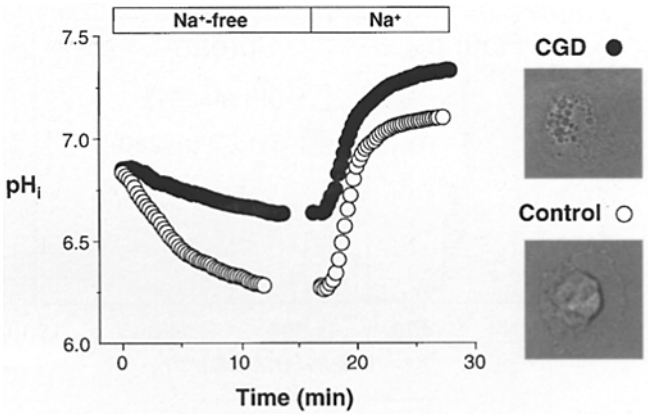

Figure 6. Acid production by control and CGD neutrophils. Time course of pH_i changes during spreading of CGD (*filled circles*) or control (*open circles*) neutrophils on glass coverslips. Where indicated, the Na^+-free solution was changed to a Na^+-rich solution. For each condition, data are means of three cells from a representative experiment. Insets illustrate the typical morphology that was observed.

To confirm the involvement of the NADPH oxidase and to quantitate the acid it generates during spreading, we used DPI, an NADPH oxidase inhibitor, and cytochalasin D, an inhibitor of actin filament assembly. Cells were preincubated for 10 min with 1 μM cytochalasin D or DPI, and were then allowed to adhere for an additional 10 min in the presence of the inhibitor. The steady-state pH_i and area of >230 cells were then determined for each condition by imaging. As illustrated in Fig. 7 (*top panel*), cytochalasin D completely inhibited spreading, yielding a homogeneous population of cells with an area <400 pixels, whereas DPI did not alter spreading, yielding the usual two-component distribution. The excess acidification induced by spreading in Na^+-free solution was completely eliminated by the oxidase inhibitor (Fig. 7, *bottom panel*, compare with Fig. 4), confirming that most, if not all, the acid produced during spreading is generated by the NADPH oxidase. Consistent with the results obtained with CGD neutrophils, DPI did not prevent the alkalinization noted in Na^+-containing medium and in fact potentiated this effect somewhat (Fig. 7). This observation rules out that DPI induces nonspecific cell damage. Interestingly, when spreading was prevented with cytochalasin D, neither the Na^+-dependent alkalinization nor the acid production were observed, suggesting that spreading and/or the associated cytoskeletal reorganization are required for the activation of both Na^+/H^+ exchange and of the NADPH oxidase in adherent neutrophils.

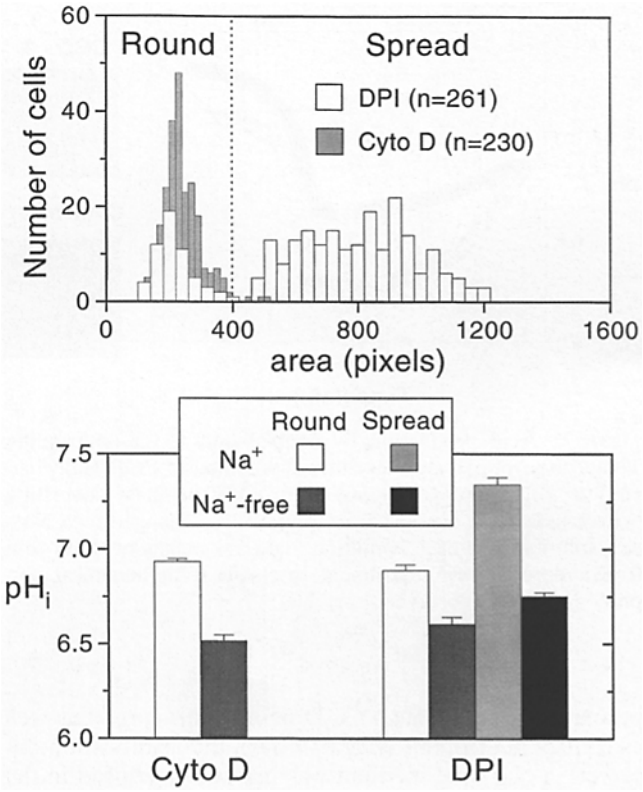

Figure 7. Acid production in cytochalasin D- and DPI-treated neutrophils. (*Top panel*) Frequency distribution of the surface area of neutrophils 10–20 min after plating on glass in the presence of either 1 μM cytochalasin D (*dark bars*) or 1 μM DPI (*open bars*). The cell areas were determined as described in Fig. 5. Neutrophils were separated into spread and round cells, where indicated by the vertical line, using the criteria developed in Fig. 5. The total number of cells traced was 230 for cytochalasin and 261 for DPI. (*Bottom panel*) Steady-state pH_i values of round and spread neutrophils, measured 10–20 min after adhesion in Na^+-containing or Na^+-free medium in the presence of either 1 μM cytochalasin D or 1 μM DPI. The cells were separated into round and spread, using the criteria developed above. For each condition, data are means ± SEM of at least 40 cells from 3–12 experiments.

Activation of Neutrophil NADPH Oxidase

The absence of acid generation in CGD and in DPI-treated neutrophils strongly suggests involvement of the respiratory burst. To confirm that the NADPH oxidase was activated under the conditions used, we measured superoxide production in single, spreading neutrophils with DHR (33). To test the ability of this probe to detect superoxide production from single cells, neutrophils from control and CGD patients were mixed and adhered to coverslips (Fig. 8, *right panels*). For identification purposes, the CGD neutrophils were loaded with Indo-1 (Fig. 8, *left panels*), the fluorescence of which does not interfere with the detection of rhodamine 123 (*Rhod 123*), the product of DHR oxidation (Fig. 8, *middle panels*). No intracellular rhodamine 123 fluorescence was observed in any of the freshly plated cells, but a bright signal was observed 20 min after plating in the control spread neutrophils. In contrast, CGD cells or the subpopulation of normal cells that failed to spread accumulated only negligible amounts of rhodamine 123 despite being plated next to superoxide-producing control cells. Thus, the superoxide or the rhodamine 123 generated by an active cell does not "spill over" significantly to neighboring cells, validating the assay of oxidase activity by fluorescence imaging.

Figs. 9 and 10 illustrate that neutrophil spreading was indeed associated with NADPH oxidase activation. On glass coverslips, rhodamine 123 fluorescence was detectable 5 min after plating in spread but not in round neutrophils, even after addition of fMLP (Figs. 9 *B* and 10, *bottom panel*). The fluorescence then increased steadily for 30 min with a time course that corresponded well to the acidification observed in Na^+-free solutions. No rhodamine 123 fluorescence was observed when spreading on glass was prevented by cytochalasin D (Fig. 9 *E*) or when cells were adhered to fibrinogen, which results in minimal spreading (Fig. 10, *top panel*). Induction of spreading on fibrinogen by the addition of chemoattractant resulted in marked accumulation of rhodamine 123 (Fig. 10, *top*). By contrast, CGD or DPI-treated neutrophils, which spread normally but lacked a functional oxidase, remained nonfluorescent throughout the experiment (Fig. 9 *F*), even after stimulation with fMLP (Fig. 10), confirming that the fluorescence increase reflected NADPH oxidase activation. Thus, conditions associated with acid production also induced NADPH oxidase activation, suggesting that the NADPH oxidase is the main source of the intracellular acid generated during neutrophil spreading.

pH Dependence of Neutrophil Spreading

While the rates of acid production and extrusion seem to be altered upon spreading, it is unclear whether the pH_i changes themselves influence the rate and extent of neutrophil spreading. To study the dependence of neutrophil spreading on pH_i, we ensured that the pH_i would remain constant at desired values as the area and shape factor were monitored microscopically (Fig. 11). To clamp pH_i, suspended neutrophils were preincubated for 5 min in nigericin-containing KCl media titrated to pH 7.0 (Fig. 11, *open circles*) or pH 6.0 (Fig. 11, *filled circles*), and then allowed to adhere and spread in the same media. The measured pH_i remained remarkably stable throughout the 20-min observation period (Fig. 11, *left panel*). Spreading occurred normally when the pH_i was held constant at 7.0, but was strongly inhibited at pH_i 6.0 (Fig. 11, *right panel*). While the shape changes at pH_i 7.0 were not different from those observed in Na^+-containing medium (see Fig. 2), at pH_i 6.0, the cells were unable to spread, although pseudopod extension was observed (Fig. 11, *inset*). This change in morphology was observed consistently and translated into a minimal increase in area and a significant decrease in the ellipsoid (shape factor) value (Fig. 11). Similar results were obtained in 88 cells from three donors. Inhibition of spreading by acidic pH_i was only observed when the cells were acidified in nigericin-containing medium before plating, i.e., when an acidic pH_i was imposed before adhesion. Without preacidification, neutrophils spread normally when plated directly in nigericin/pH 6.0 solutions despite the rapid (<2 min) acidification of the cytosol to pH ~6.0 (not shown). Thus, the initial phase of cellular spreading, but not maintenance of the spread state, appear to be in-

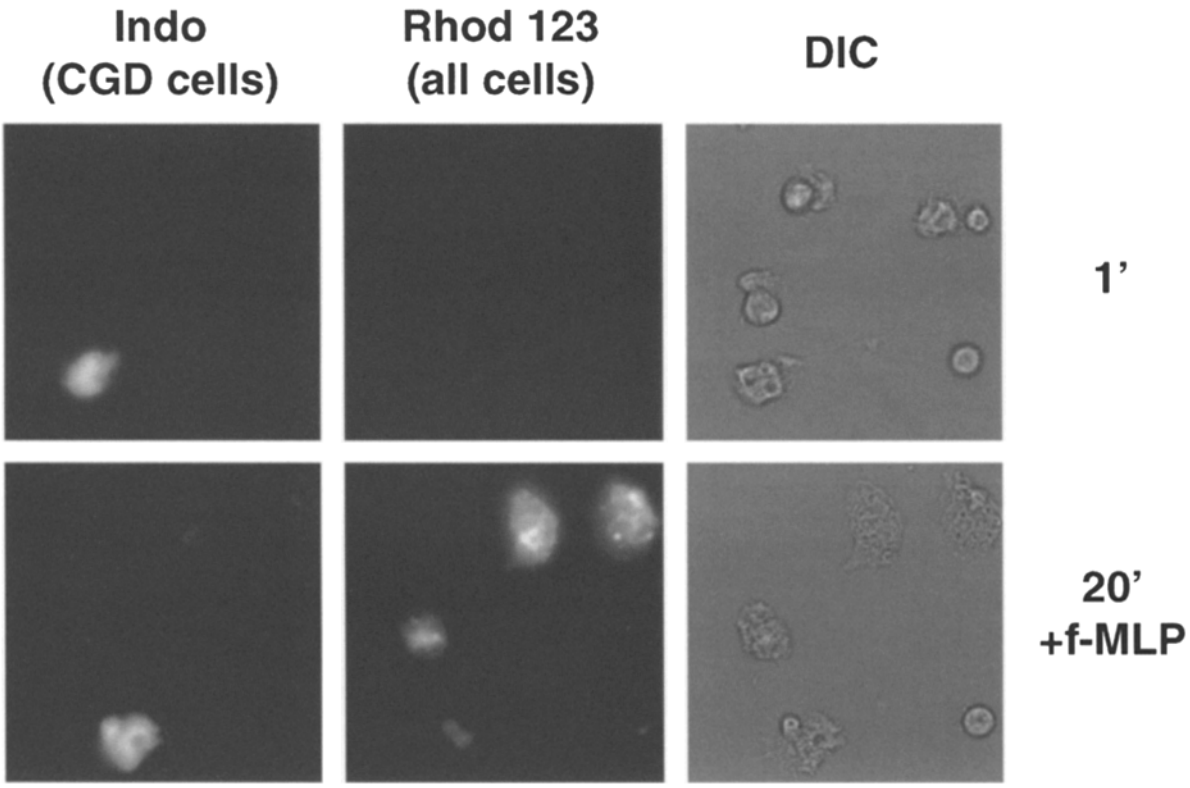

Figure 8. Measurements of superoxide production in single adherent neutrophils. Simultaneous imaging of Rhod123 and Indo-1 fluorescence in adherent neutrophils. Cells from a CGD donor were loaded with Indo-1 and mixed with unloaded normal neutrophils. The cells were allowed to adhere on fibrinogen-coated glass while continuously perfused with the nonfluorescent substrate dihydrorhodamine 123 (*DHR*), the reduced precursor of rhodamine 123. After 2 min, the cells were stimulated with 1 μM fMLP. At 1 and 20 min, rhodamine 123 fluorescence was measured with excitation at 490 nm (*A* and *C*), while the Indo-1 fluorescence identifying CGD neutrophils was detected with excitation at 360 nm (*B* and *D*). Emission was measured at 535 ± 25 nm.

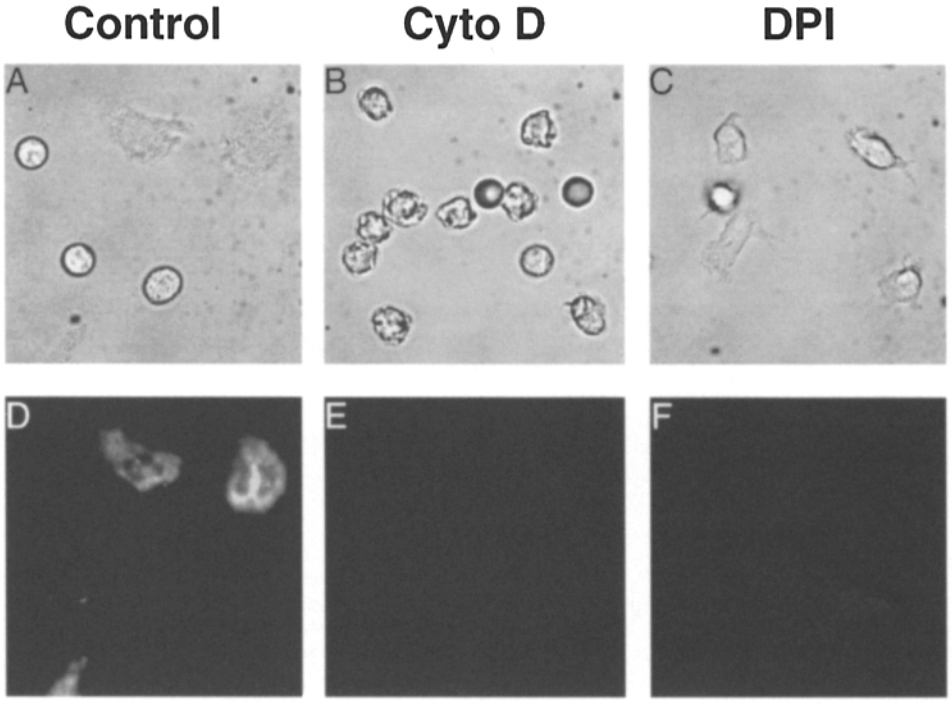

Figure 9. Spreading activates neutrophil NADPH oxidase. Bright-field (*A–C*) and Rhod123 fluorescence (*D–F*) imaging of neutrophils 20 min after adherence to glass coverslips while bathed in standard (Na^+-containing) solution. Where noted, the incubation solution contained 1 μM cytochalasin D or 1 μM DPI. Rhod123 fluorescence was imaged as described in Fig. 6. Images shown are representative of three to eight experiments for each condition.

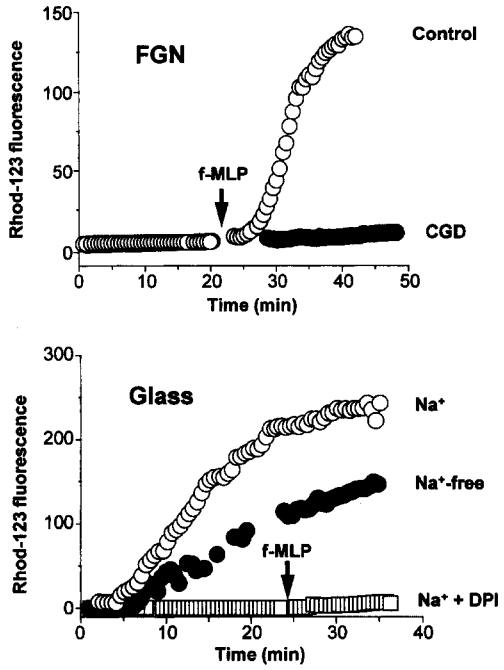

Figure 10. Time course of spreading-induced oxidase activation. Changes in Rhod123 fluorescence during neutrophil spreading on fibrinogen or glass coverslips. (*A*) CGD (*filled circles*) and control (*open circles*) neutrophils were adhered to fibrinogen-coated coverslips and stimulated with fMLP (10^{-6} M, *arrow*). (*B*) Neutrophils were adhered to glass coverslips in Na^+-free medium (*solid circles*) or in Na^+-medium in the absence (*open circles*) or presence of 1 μM DPI (*squares*). Where indicated, fMLP (1 μM) was added to the samples containing DPI. The fluorescence of Rhod123 was imaged over time as described in Fig. 7 and then quantified. For each condition, the Rhod123 fluorescence intensity of three to five neutrophils was averaged.

hibited by acidic pH_i. This explains why the acidification observed in Na^+-free medium does not fully inhibit spreading by itself (Fig. 2).

The constancy of pH_i during the course of spreading in nigericin/K^+-containing media despite rapid and large shape alterations further supports the validity of the pH_i changes measured in the absence of the ionophore.

Discussion

Our results demonstrate that neutrophils undergo pronounced and consistent changes in pH_i during the course of adherence and spreading. In physiological, Na^+-rich solutions, the cells rapidly alkalinize by 0.2–0.3 pH units. This pH_i increase occurs despite an underlying increase in H^+ (equivalent) production, which reflected the activation of the respiratory burst. The concomitant activation of the NADPH oxidase and pH_i regulatory mechanisms can be mediated by the adherence receptors of the β2-integrin family, since pH_i changes were observed on coverslips coated with an anti-CD18 mAb (Fig. 3 *A*), whereas incubation with a soluble anti-CD18 mAb markedly reduced the changes observed on fibrinogen (Fig. 3 *B*). Regardless of the substrate, increased H^+ production and export were always associated with the morphological changes that are characteristic of spreading. Neutrophils that remained

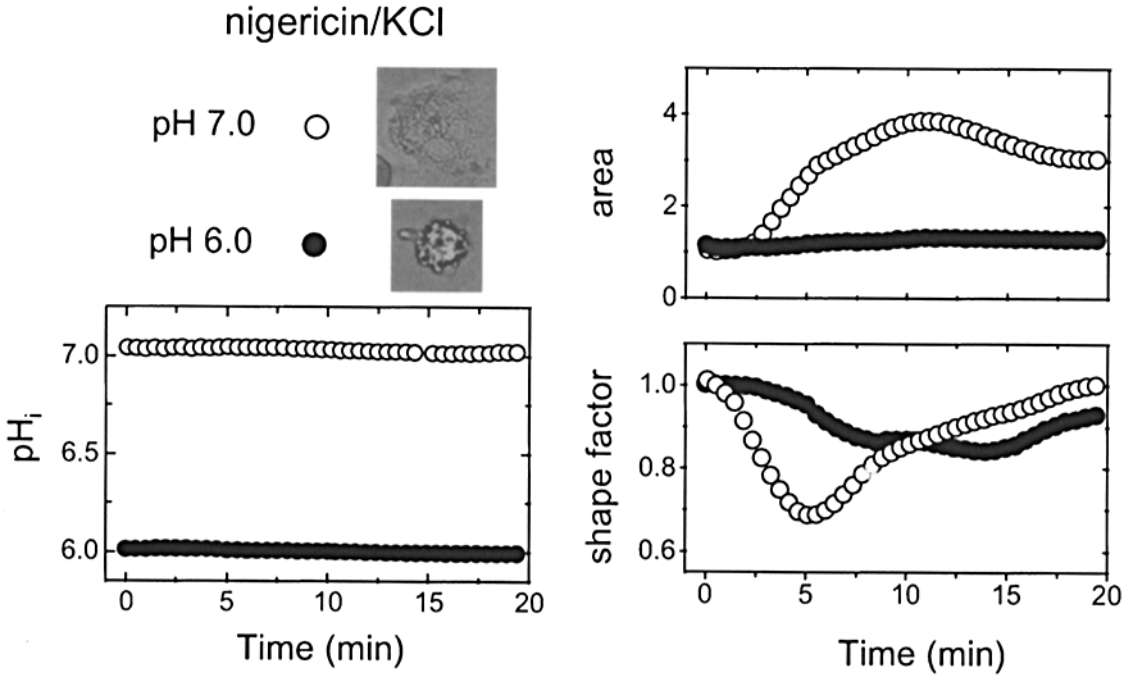

Figure 11. Effect of pH_i on neutrophil spreading. Neutrophils were preequilibrated for 5 min in nigericin-containing K^+-rich media of pH 7.0 (*open circles*) or pH 6.0 (*solid circles*). The cells were then plated on glass (time 0 in figure) in the same media, and their pH_i (*graph at bottom left*), area (*top right*) and shape factor (*bottom right*) were monitored as in Fig. 2 for the next 20 min. The two representative cells used to plot the graphs are illustrated in the top left insets.

round, such as the subpopulation of cells that failed to spread on glass coverslips, those treated with cytochalasin D, or the cells that adhered to fibrinogen but were not induced to spread, did not produce superoxide and maintained a constant pH_i. This spreading-associated activation might reflect the increased number of adherence receptors engaged in a spread neutrophil compared to a round neutrophil. Alternatively, cytoskeletal reorganization might be required to activate the respiratory burst and H^+ metabolism, since the cytosolic oxidase components $p47^{phox}$ and $p67^{phox}$, as well as NHE-1, the ubiquitous isoform of the antiporter, have been shown to associate with the cytoskeletal structures (18, 23). The integrin-mediated activation of Na^+/H^+ exchange in adherent neutrophils seemingly requires extensive cytoskeletal remodeling, since cross-linking of saturating concentrations of anti-integrin antibodies in suspended neutrophils is not a sufficient stimulus to activate Na^+/H^+ exchange (20).

The activation of the respiratory burst during the course of cell spreading appeared responsible for most of the excess H^+ production, resembling the reported acidification of suspended cells in which the NADPH oxidase was maximally activated using phorbol esters (21). The conclusion that the oxidase reaction itself or the associated stimulation of the hexose monophosphate shunt generates sufficient metabolic acid equivalents to account for the drop in pH_i is supported by (*a*) the failure of CGD neutrophils to acidify; (*b*) the inhibitory effects of DPI; and (*c*) the close correlation between acid production and superoxide generation measured with rhodamine 123 (see Table I for summary).

Despite the exaggerated rate of H^+ generation, pH_i in fact increases during spreading in physiological medium. This is attributable to the activation of pH_i regulatory systems. Three main H^+ (equivalent) transporters operate in neutrophils suspended in nominally bicarbonate-free media: Na^+/H^+ exchangers, an H^+-selective conductance, and H^+ pumps (for review see reference 7). The latter seem to contribute little to regulation in spreading cells, since inhibitory concentrations of bafilomycin had little effect on pH_i (not shown). An H^+ conductance, in contrast, is demonstrably active in spreading cells. As illustrated in Fig. 5, addition of Zn^{2+}, a potent blocker of neutrophil H^+ conductance (11, 12), to cells that acidified in the presence of HOE 694 caused a further acidification of ~0.1 pH units. This suggests that net H^+ efflux through the conductive pathway partially compensated the tendency of spreading neutrophils to acidify. Further confirmation of the postulated role of this conductance in neutrophil activation (13) would require electrophysiological recording from spreading neutrophils.

Na^+/H^+ exchange is by far the largest contributor to H^+ extrusion in activated neutrophils. This was revealed by the occurrence of a large acidification when cells spread in Na^+-free media or in Na^+-rich solutions containing inhibitors of the antiport, such as HOE 694 (e.g., Fig. 5). The rate and directionality of the antiporter depend on the prevailing Na^+ gradient: at high external [Na^+], H^+ efflux through the antiporter overcompensated for the acid generated by the oxidase, resulting in a net cytosolic alkalinization. In the absence of extracellular Na^+, not only did acid accumulate because of metabolic generation, but additional H^+ entered the cell through the antiporter, which operated in the reverse mode under these conditions, further compounding the acid load. It is noteworthy that the antiporter was activated in response to spreading and not to the metabolic acidosis (Table I). This is indicated by three findings: (*a*) the pH_i of spread cells overshot the basal level; (*b*) the onset of the alkalinization preceded the respiratory burst; and (*c*) an even greater alkalinization was observed in CGD neutrophils and in DPI-treated cells, where the acidifying component was missing. Thus, activation of Na^+/H^+ exchange was not driven by the excess internal substrate, but was a direct consequence of spreading.

Table I. Correlation between Spreading, Superoxide, and pH Changes

Condition	Substrate	Spreading	Na^+/H^+ exchange	Acid production	O_2^- production
Control	Glass	+	+	+	+
Control	IB4	+	+	+	+
Control	FGN	−	−	−	−
fMLP	FGN	+	+	+	+
HOE	Glass	+	−	+	+
DPI	Glass	+	+	−	−
CGD	Glass	+	+	−	−
Cyto D	Glass	−	−	−	−

Neutrophil spreading proceeded when either the oxidase or the antiporter were blocked (Figs 4–7 and Table I), and also when pH_i was clamped near physiological values with nigericin (Fig. 11). This implies that pH_i changes are not essential signals for neutrophil spreading. On the other hand, the ability of neutrophils to spread seems to be modulated by pH_i, since spreading was strongly inhibited when an acidic pH_i was imposed using nigericin (Fig. 11). Interestingly, the inhibition of spreading required preacidification of the cells, since neutrophils spread normally when acidified shortly after contact with the substrate. This suggests that the pH-sensitive step is an early event, and that adherence and spreading, once initiated, can proceed independently of pH_i.

In summary, our results demonstrate that neutrophils release superoxide upon spreading, and that this process is associated with a burst of intracellular acid generation. Despite this increased acid production, a net cytosolic alkalinization is observed when the cells are bathed in physiological (Na^+-rich) medium, mainly as a result of concomitant activation of the Na^+/H^+ antiport. Under these conditions, the H^+ conductive pathway and H^+-ATPases contribute comparatively less to acid extrusion. However, as neutrophils are exposed to media of differing ionic composition when they perform their microbicidal functions, the H^+ conductance and the ATPase might act as safeguard mechanisms, allowing H^+ extrusion in acidic, low Na^+ environments such as abscesses, which are thermodynamically unfavorable for Na^+/H^+ exchange. Finally, the main role of the H^+ transporting systems appears to be in cellular homeostasis and not in signaling: spreading and the respiratory burst do not require the activity of cellular H^+ channels or exchangers and proceed normally when pH_i is stabilized near the physiological value by exogenous means (e.g., nigericin/K^+). On the other hand, inhibition of pH_i

regulation by interference with the endogenous transporters results in drastic acidification, with resultant impairment of neutrophil function.

This research was funded by operating grants awarded to S. Grinstein and G.P. Downey by the Medical Research Council of Canada. N. Demaurex is supported by the Swiss National Research Council. G.P. Downey is the recipient of an Ontario Ministry of Health Career Scientist award. T.K. Waddell is the recipient of a Medical Research Council of Canada Fellowship. S. Grinstein is cross-appointed to the Department of Biochemistry of the University of Toronto and is an International Scholar of the Howard Hughes Medical Institute.

Received for publication 19 October 1995 and in revised form 8 February 1996.

References

1. Babior, B.M. Oxygen-dependent microbial killing by phagocytes. 1978. *N. Engl. J. Med.* 12:659–668.
2. Bengtsson, T., M.E. Jaconi, M. Gustafson, K.E. Magnusson, J.M. Theler, D.P. Lew, and O. Stendahl. 1993. Actin dynamics in human neutrophils during adhesion and phagocytosis is controlled by changes in intracellular free calcium. Eur. J. Cell Biol. 62:49–58.
3. Berton, G., C. Laudanna, C. Sorio, and F. Rossi. 1992. Generation of signals activating neutrophils functions by leukocyte integrins: LFA-1 and gp150/95, but not CR3, are able to stimulate the respiratory burst of human neutrophils. *J. Cell Biol.* 116:1007–1017.
4. Borregaard, N., J.H. Schwartz, and A.I. Tauber. 1984. Proton secretion by stimulated neutrophils. Significance of hexose monophosphate shunt activity as source of electrons and protons for the respiratory burst. *J. Clin. Invest.* 74:455–459.
5. Boyum, A. 1968. Isolation of mononuclear cells and granulocytes from human blood. *Clin. Lab. Invest.* 21:77–98.
6. Brundage, R.A., K.E. Fogarty, R.A. Tuft, and F.S. Fay. 1991. Calcium gradients underlying polarization and chemotaxis of eosinophils. *Science (Wash. DC).* 254:703–706.
7. Chow, C.W.C., N. Demaurex, and S. Grinstein. 1995. Ion transport and the function of phagocytic cells. *Curr. Opin. Hematol.* 2:89–95.
8. Clark, R.A. 1990. The human respiratory burst oxidase. *J. Infect. Dis.* 161: 1140–1147.
9. Collette, J., D. McGreer, R. Crawford, F. Chubb, and R.D. Sandin. 1956. Synthesis of some cyclic iodonium salts. *J. Am. Chem. Soc.* 78:3819–3820.
10. Counillon, L., W. Scholz, H.J. Lang, and J. Pouysségur. 1993. Pharmacological characterization of stably transfected Na^+/H^+ antiporter isoforms using amiloride analogs and a new inhibitor exhibiting anti-ischemic properties. *Mol. Pharmacol.* 44:1041–1045.
11. DeCoursey, T.E., and V.V. Cherny. 1993. Potential, pH, and arachidonate gate hydrogen ion currents in human neutrophils. *Biophys. J.* 65:1590–1598.
12. Demaurex, N., S. Grinstein, M. Jaconi, W. Schlegel, D.P. Lew, and K.H. Krause. 1993. Proton currents in human granulocytes: regulation by membrane potential and intracellular pH. *J. Physiol.* 466:329–344.
13. Demaurex, N., J. Schrenzel, M.E. Jaconi, D.P. Lew, and K.H. Krause. 1993. Proton channels, plasma membrane potential, and respiratory burst in human neutrophils. *Eur. J. Haematol.* 51:309–312.
14. Downey, G.P., C.K. Chan, P. Lea, A. Takai, and S. Grinstein. 1992. Phorbol ester-induced actin assembly in neutrophils: role of protein kinase C. *J. Cell Biol.* 116:695–706.
15. Downey, G.P. 1994. Mechanisms of leukocyte motility and chemotaxis. *Curr. Opin. Immunol.* 6:113–124.
16. Deleted in proof.
17. Edmonds, B., J. Murray, and J. Condeelis. 1995. pH regulation of the F-actin binding properties of *Dictyostelium* elongation factor 1a. *J. Biol. Chem.* 270:15222–15230.
18. El Benna, J., J.M. Ruedi, and B.M. Babior. 1994. Cytosolic guanine nucleotide-binding protein Rac2 operates in vivo as a component of the neutrophil respiratory burst oxidase. Transfer of Rac2 and the cytosolic oxidase components $p47^{phox}$ and $p67^{phox}$ to the submembranous actin cytoskeleton during oxidase activation. *J. Biol Chem.* 269:6729–6734.
19. Foskett, J.K. 1988. Simultaneous Nomarski and fluorescence imaging during video microscopy of cells. *Am J. Physiol.* 248:C27–C36.
20. Fukushima, T., T.K. Waddell, S. Grinstein, G.G. Gross, J. Orlowski, and G.P. Downey. 1996. Na^+/H^+ exchange activity during phagocytosis in human neutrophils: Role of Fcγ receptors and tyrosine kinases. *J. Cell Biol.* 132:1037–1052.
21. Grinstein, S., and W. Furuya. 1986. Cytoplasmic pH regulation in phorbol ester-activated human neutrophils. *Am. J. Physiol.* 251:C55–C65.
22. Grinstein, S., W. Furuya, and W.D. Biggar. 1986. Cytoplasmic pH regulation in normal and abnormal neutrophils. Role of superoxide generation and Na^+/H^+ exchange. *J. Biol. Chem.* 261:512–514.
23. Grinstein, S., M. Woodside, T.K. Waddell, G.P. Downey, J. Orlowski, J. Pouyssegur, D.C.P. Wong, and J.K. Foskett. 1993. Focal localization of the NHE-1 isoform of the Na^+/H^+ antiport. Assessment of effects on intracellular pH. *EMBO (Eur. Mol. Biol. Organ.) J.* 12:5209–5218.
24. Henderson, L.M., J.B. Chappell, and O.T.G. Jones. 1988. Internal pH changes associated with the activity of NADPH oxidase of human neutrophils. Further evidence for the presence of an H^+-conducting channel. *Biochem. J.* 251:563–567.
25. Hendey, B., and F.R. Maxfield. 1993. Regulation of neutrophil motility and adhesion by intracellular calcium transients. *Blood Cells.* 19:143–161.
26. Jaconi, M.E., J.M. Theler, W. Schlegel, R.D. Appel, S.D. Wright, and P.D. Lew. 1991. Multiple elevations of cytosolic-free $Ca2^+$ in human neutrophils: initiation by adherence receptors of the integrin family. *J. Cell Biol.* 112:1249–1257.
27. MacFarlane, G.D., M.C. Herzberg, and R.D. Nelsøn. 1987. Analysis of polarization and orientation of human polymorphonuclear leukocytes by computer-interfaced video microscopy. *J. Leukocyte. Biol.* 41:307–317.
28. Mandeville, J.T., R.N. Ghosh, and F.R. Maxfield. 1995. Intracellular calcium levels correlate with speed and persistent forward motion in migrating neutrophils. *Biophys. J.* 68:1207–1217.
29. Marks, P.W., and F.R. Maxfield. 1990. Transient increases in cytosolic free calcium appear to be required for the migration of adherent human neutrophils. *J. Cell Biol.* 110:43–52.
30. Nathan, C., S. Srimal, C. Farber, E. Sanchez, L. Kabbash, A. Asch, J. Gailit, and S.D. Wright. 1989. Cytokine-induced respiratory burst of human neutrophils: dependence on extracellular matrix proteins and CD11/CD18 integrins. *J. Cell Biol.* 109:1341–1349.
31. Pozzan, T., D. Lew, C. Wollheim, and R.Y. Tsien. 1983. Is cytosolic ionized calcium regulating neutrophil activation? *Science (Wash. DC).* 221:1413–1415.
32. Roos, A., and W.F. Boron. 1981. Intracellular pH. *Physiol. Rev.* 61:296–434.
33. Rothe, G., A. Oser, and G. Valet. 1988. Dihydrorhodamine 123: a new flow cytometric indicator for respiratory burst activity in neutrophil granulocytes. *Naturwissenschaften.* 75:354–355.
34. Simchowitz, L. 1985. Chemotactic factor-induced activation of Na^+/H^+ exchange in human neutrophils. II. Intracellular pH changes. *J. Biol. Chem.* 260:13248–13255.
35. Simchowitz, L., and E.J. Cragoe, Jr. 1986. Regulation of neutrophil chemotaxis by intracellular pH. *J. Biol. Chem.* 261:6492–6500.
36. Smith, R.M., and J.T. Curnutte. 1991. Molecular basis of chronic granulomatous disease. *Blood.* 77:673–686.
37. Springer, T.A. 1990. Adhesion receptors of the immune system. *Nature (Lond.).* 346:425–434.
38. Stossel, T.P. 1993. On the crawling of animal cells. *Science (Wash. DC).* 260:1086–1094.
39. Theler, J.M., D.P. Lew, M.E. Jaconi, K.H. Krause, C.B. Wollheim, and W. Schlegel. 1995. Intracellular pattern of cytosolic Ca^{2+} changes during adhesion and multiple phagocytosis in human neutrophils. Dynamics of intracellular Ca^{2+} stores. *Blood.* 85:2194–2201.
40. Thomas, J.A., R.N. Buchsbaum, A. Zimniak, and E. Racker. 1982. Intracellular pH measurements in Ehrlich ascites tumor cells utilizing spectroscopic probes generated in situ. *Biochemistry.* 18:2210–2218.
41. Tsien, R.Y. 1989. Fluorescent indicators of ion concentrations. *In* Fluorescence Microscopy of Living Cells in Culture. Part B. Y.L. Wand and D.L. Taylor, editors. Academic Press, Inc., San Diego, CA 127–156.